

Molecular Modeling of Saccharides, Part 25[†]Structure and Lipophilicity Profile of 2,3-Anhydro- α -cyclomannin** and Its Ethanol Inclusion ComplexStefan Immel,^[a] Kahee Fujita,^[b] Hans J. Lindner,^[a] Yasuyoshi Nogami,^[c] and Frieder W. Lichtenthaler*^[a]

Abstract: Readily available from α -cyclodextrin in three steps, 2,3-anhydro- α -cyclomannin composed of six α -(1 \rightarrow 4)-linked 2,3-anhydro-D-mannopyranose residues, crystallizes well when precipitated from aqueous ethanol. An X-ray structure reveals the macrocycle to contain ethanol in its cavity, thus representing the first inclusion complex of a non-glucose cyclooligosaccharide. The wider rim of the torus-shaped macrocycle holds the six epoxide rings whose oxygens point away from the cavity, thereby sculpturing the unique over-all shape of a six-pointed star.

Keywords: α -2,3-anhydro- α -cyclomannin \cdot α -cyclodextrin \cdot cyclooligosaccharides \cdot inclusion complexes

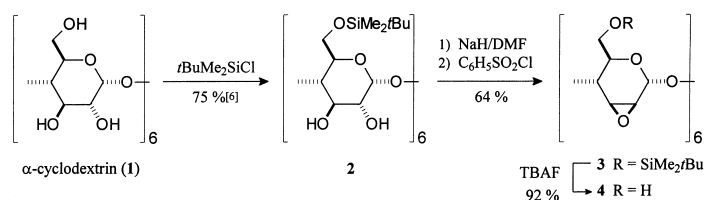
Introduction

Cyclooligosaccharides composed of sugars other than glucose have gained considerable interest recently, as they are apt to provide host molecules with recognition features different from those of the rigid cyclodextrins.^[1] However, despite of sufficiently hydrophobic CD-like cavities in the case of the cyclomannins,^[2] 2,3-anhydro-cyclomannins,^[3–5] cyclorhamnins,^[1a] various analogues with alternating D-mannose/L-mannose and D-mannose/L-rhamnose residues,^[6] and the conformationally flexible cycloaltrins,^[7, 8] indications of their

interaction with suitable guests are exceedingly scarce: 2,3-anhydro- α -cyclomannin, based on sparse ¹H-NMR data, seems to be able to incorporate 4-nitrophenol,^[3a, 9] and the cycloaltrins, on equally scant capillary electrophoretic evidence, appear capable of interacting with sodium 4-*tert*-butylbenzoate.^[8] It is in this context, that here, with the X-ray-based unravelment of the unique molecular architecture of the title compound, we provide unequivocal proof for the first inclusion complex of a non-glucose cyclooligosaccharide.

Results and Discussion

Synthesis: Our synthetic approach to 2,3-anhydro- α -cyclomannin,^[4] as illustrated in Scheme 1, started from α -cyclodextrin by protection of the six primary hydroxyl groups by



Scheme 1. Synthesis of 2,3-anhydro- α -cyclomannin (4) from α -cyclodextrin (1).

the *tert*-butyl-dimethylsilyl moiety (\rightarrow 2^[6]). Ensuing deprotonation of the secondary hydroxyls in 2 by treatment with NaH in DMF was followed by the addition of benzenesulfonyl chloride, which not only effected selective 2-*O*-sulfonylation

[a] Prof. Dr. F. W. Lichtenthaler, Dr. S. Immel, Prof. Dr. H. J. Lindner
Institut für Organische Chemie, Technische Universität Darmstadt
Petersenstrasse 22, 64287 Darmstadt (Germany)
Fax: (+49) 6151-166674
E-mail: fwlicht@sugar.oc.chemie.tu-darmstadt.de

[b] Prof. Dr. K. Fujita
Faculty of Pharmaceutical Sciences, Nagasaki University
Nagasaki 852-8131 (Japan)

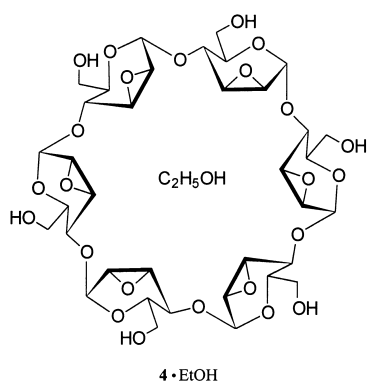
[c] Prof. Dr. Y. Nogami
Daiichi College of Pharmaceutical Sciences
Fukuoka 815 (Japan)

[†] Presented in part at the XVIIth Japanese Cyclodextrin Symposium, Osaka, October 1999.—Part 24: S. Immel, F. W. Lichtenthaler, *Stärke* **2000**, 52, 1–8.

[**] A cyclooligosaccharide composed of six α -(1 \rightarrow 4)-linked 2,3-anhydro-D-mannopyranose units; for terminology used see ref. [5].

Supporting information for this article is available on the WWW under <http://caramel.oc.chemie.tu-darmstadt.de/imm/3Dstructures.html> (3D structures of Figure 1) and <http://caramel.oc.chemie.tu-darmstadt.de/imm/molcad/gallery.html> (MOLCAD graphics).

but, concomitantly, displacement of the 2-sulfonyloxy group by the vicinal 3-OH to elaborate the 6-*O*-protected 2,3-anhydro- α -cyclomannin (**3**, 64%). Deblocking with TBAF/THF proceeded smoothly (4 h, 40 °C) and led after crystallization from aqueous ethanol to a product in 84% yield, which, however, was not the free 2,3-anhydro- α -cyclomannin (**4**), but its ethanol inclusion complex $4 \cdot C_2H_5OH$ with varying amounts of water. An intensively dried sample analyzed for the dihydrate, the crystal grown and used for the X-ray structural analysis revealed $4 \cdot C_2H_5OH$ to be associated with $3.5H_2O$ on the average (vide infra).



X-ray Structure: That the 2,3-anhydro- α -cyclomannin accumulated as the ethanol inclusion complex when crystallized from aqueous ethanol could neither be proved by mass spectral data—the complex does not survive the high vacuum MS conditions as only the $[M]^+$ peak for the cyclooligosaccharide is detectable—nor by 1H - or ^{13}C -NMR spectroscopy, since in $[D_5]$ pyridine solution it is unclear whether the ethanol-CH protons or its carbon atoms are inside or outside the cavity, in fact, the formation of a pyridine inclusion

complex being not unlikely. Only the X-ray structural analysis, invited by the high crystallinity of the product, revealed the ethanol to be located in the interior of the cavity (Figure 1). The geometry of the complex unfolds a high degree of regularity, with the backbone of the macrocycle best approximated by six-fold rotational symmetry (C_6). All epoxide rings are lined up on one side of the torus-shaped molecule—the larger aperture in fact—and point away from the center molecular axis towards the outside of the macro-ring. These structural features result in the unique over-all shape of a six-pointed star (Figure 1).

The intersaccharidic torsion angles Φ (O5-C1-O1-C4') and ψ (C1-O1-C4'-C3') show only small fluctuations (94.2 ± 2.9 and $123.3 \pm 9.4^\circ$, respectively), as do the atomic distances O1–O1 diagonally across the ring ($8.74 \pm 0.26 \text{ \AA}$). The pyranose units are slightly tilted with their 6-OH towards the center axis, with tilt angles^[11] of $\approx 110.2 \pm 7.7^\circ$. Table 1 records further characteristics such as the Cremer–Pople ring puckering parameters,^[12] the pyranose conformation, and selected torsion angles, revealing nearly ideal 0H_5 half-chair conformations, in which O-5 and C-5 are located above and below the mean-plane of the pyranoid rings, respectively. This implies an essentially planar arrangement of C-1 to C-4, as expressed in the very small value ($0.5 \pm 3.4^\circ$) for the C1-C2-C3-C4 torsion angle. In Table 1, these geometry descriptors are compared with those found in the solid-state structure of methyl 2,3-anhydro-4,6-di-*O*-(*p*-bromobenzyl)- α -D-mannopyranoside (**5**),^[13] whose 0H_5 pyranoid ring conformation closely resembles that found in **4**. The primary 6-OH groups adopt *gauche-trans* (*gt*, $\omega \approx +60^\circ$) and *gauche-gauche* (*gg*, $\omega \approx -60^\circ$) relative to the pyranoid ring, that is either point towards the center of the cavity (*gt*) or away from it (*gg*).

As illustrated by the space-filling model in Figure 1 and, more lucidly, by the side-view plots therein, the ethanol guest

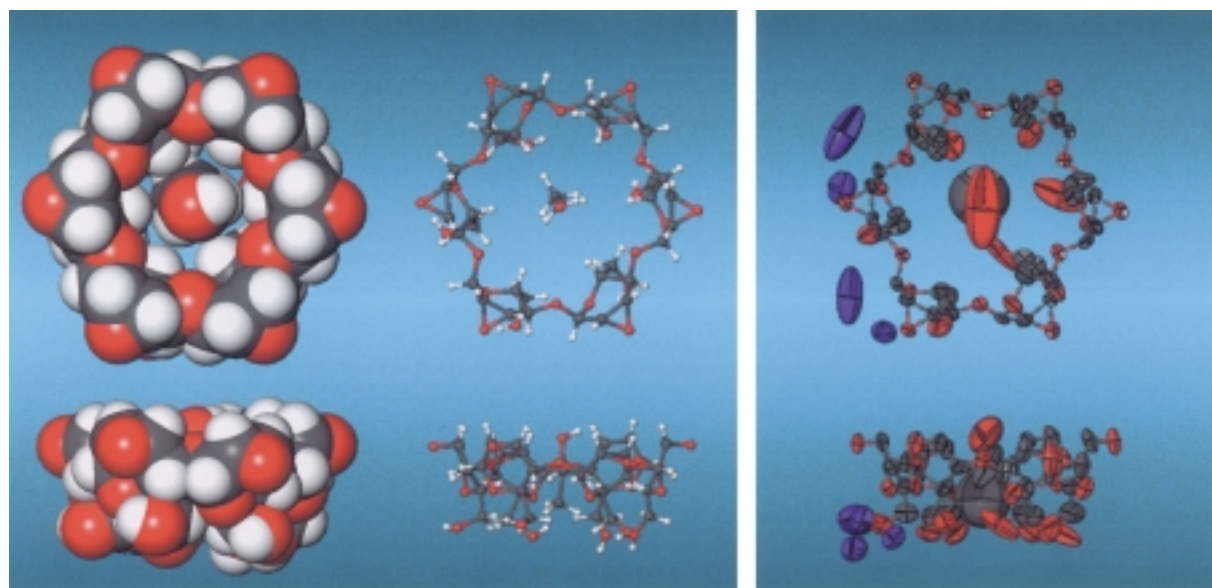


Figure 1. Molecular geometry of the 2,3-anhydro- α -cyclomannin–ethanol complex ($4 \cdot EtOH$) in the solid-state. Left and center: Space-filling and ball-and-stick models are shown perpendicular (top) and parallel (bottom) to the ring plane of the macrocycle; the water of crystallization and disorderings were omitted for clarity. Right: The anisotropic thermal 50% probability ellipsoids for all non-hydrogen atoms (blue: oxygen atoms of water molecules); two 6- CH_2OH groups (2,3-anhydro-cyclomannoside units at top left and bottom right) are statistically disordered over two sites with equal weights.

Table 1. Cremer–Pople ring puckering parameters,^[12] pyranose conformations, and selected torsion angles in the solid-state structures of the 2,3-anhydro- α -cyclomannin–ethanol complex (**4**·EtOH) compared with those of methyl 4,6-di-*O*-(*p*-bromobenzyl)-2,3-anhydro- α -D-mannopyranoside (**5**).^[13]

	4 ^[a]	5 ^[b]
Cremer–Pople parameters		
Q [Å]	0.488 (0.02)	0.517
θ [°]	51.1 (2.6)	48.1
ϕ [°]	337.8 (4.9)	335.0
pyranose conformation		
ring torsion angles [°]	oH_5	oH_5
O5–C1–C2–C3	20.2 (4.0)	21.2
C1–C2–C3–C4	0.5 (3.4)	–3.2
C2–C3–C4–C5	10.7 (3.2)	15.8
C3–C4–C5–O5	–41.0 (2.5)	–47.3
C4–C5–O5–C1	67.2 (1.6)	71.5
C5–O5–C1–C2	–55.4 (3.2)	–56.5
other torsions		
O1–C1–C2–O2	–170.5 (2.5)	–170.2
O5–C1–C2–O2	–46.4 (3.4)	–49.5
O5–C5–C6–O6	69.5 (5.7) ^[c]	71.1
	–59.2 (3.7) ^[c]	

[a] Root-mean-square (RMS) deviations in parenthesis. [b] Single parameters without RMS values. [c] Independently averaged values for the *gauche*–*trans* ($\omega \approx +60^\circ$) and *gauche*–*gauche* ($\omega \approx -60^\circ$) arrangements of the 6-CH₂OH groups.

is fully immersed into the host, with its OH-group located at the wider opening of the funnel-shaped cavity, that is the side carrying the six epoxide rings (Figure 2). As these point away from the cavity, there is no possibility of elaborating a guest–host hydrogen bond, engendering a pronounced mobility of the ethanol oxygen perpendicular to the central axis of the host (cf. thermal ellipsoids in Figure 1, right).

In the crystal lattice, the 2,3-anhydro- α -cyclomannin–ethanol complex forms layered structures that are complex yet architecturally appealing: Two units of the inclusion complex are “fused together” to head-to-head dimers with the wider, oxirane ring-bearing sides facing each other (Figure 3)—an arrangement obviously favored by the elaboration of an intense hydrogen bond between the entrapped ethanol OH-groups (O...O distance 3.03 Å). Each layer of these dimeric units is separated by a layer of water molecules (Figure 3), which are engaged in hydrogen bonding interactions with the primary 6-hydroxyls.

A detailed schematic plot of the hydrogen bonding patterns between the 6-OH groups and the water molecules is given in Figure 4; the corresponding geometry parameters are listed in Table 2. Although all hydroxyl groups and water molecules are engaged in at least two hydrogen bonds, neither the oxirane oxygens O-2 nor the pyranose ring oxygens O-5 are involved as acceptors in this network, and therefore these hydrogen-bonding patterns extend only along the layers without being interconnected in three dimensions. In addition, no hydrogen bond is observed between the ethanol guest molecule and the cyclomannin host.

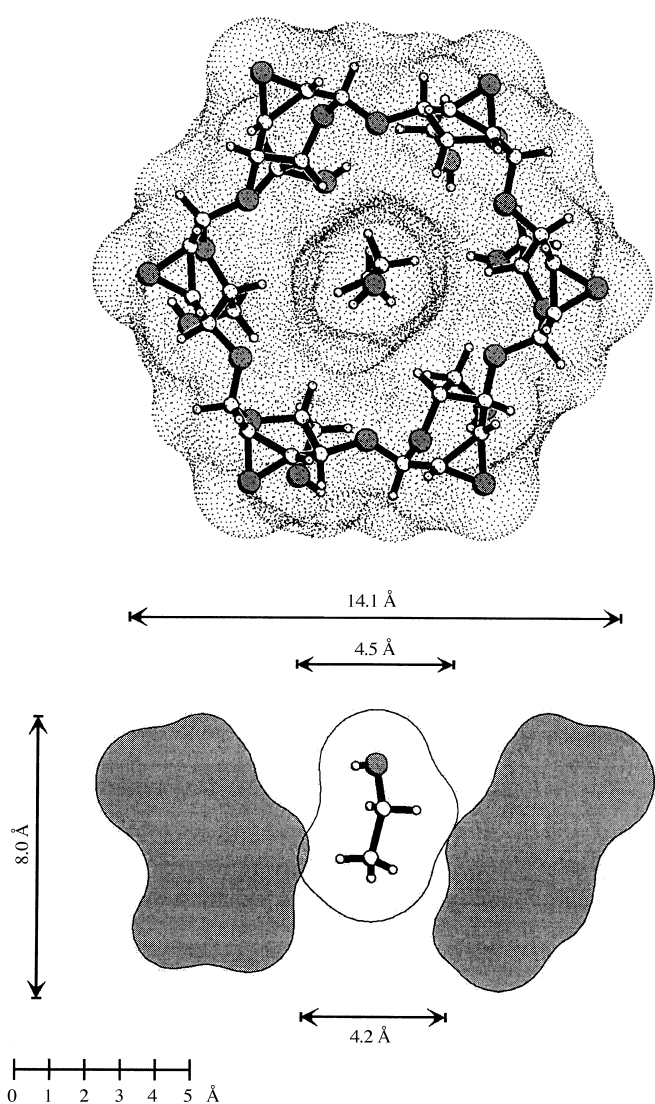


Figure 2. Top: Ball-and-stick representation of the 2,3-anhydro- α -cyclomannin–ethanol complex (**4**·EtOH) with the solvent accessible surface superimposed in dotted form; the wider opening carrying the oxirane rings is in front, the 6-CH₂OH side at rear. Bottom: Side-view surface slice, illustrating the funnel-shaped cavity and the orientation of the guest ethanol (2-O atoms at top, 6-CH₂OH face of the macrocycle at bottom); approx. molecular dimensions are included in Å.

Table 3 provides a list of some selected intermolecular atomic distances: The shortest cyclomannin host–host distances of around 3.2–3.3 Å indicate a tight packing between the molecules of each layer, as well as between the stacked macrocycles. The shortest distances between the ethanol molecules and their hosts are in the range of about 4.2–4.6 Å, thus leaving space for some thermal motions of the guests. The short O...O-distance of ≈ 3.03 Å between two symmetry related ethanol molecules is consistent with an hydrogen bond (vide supra), whereas the terminal methyl groups are separated by as much as 6.82 Å across two layers.

Lipophilicity distribution: Whilst the cavity dimensions of 2,3-anhydro- α -cyclomannin (**4**) are close to those of α -cyclodextrin, the proportion of hydrophilic and hydrophobic surface regions is to be substantially different. Simple

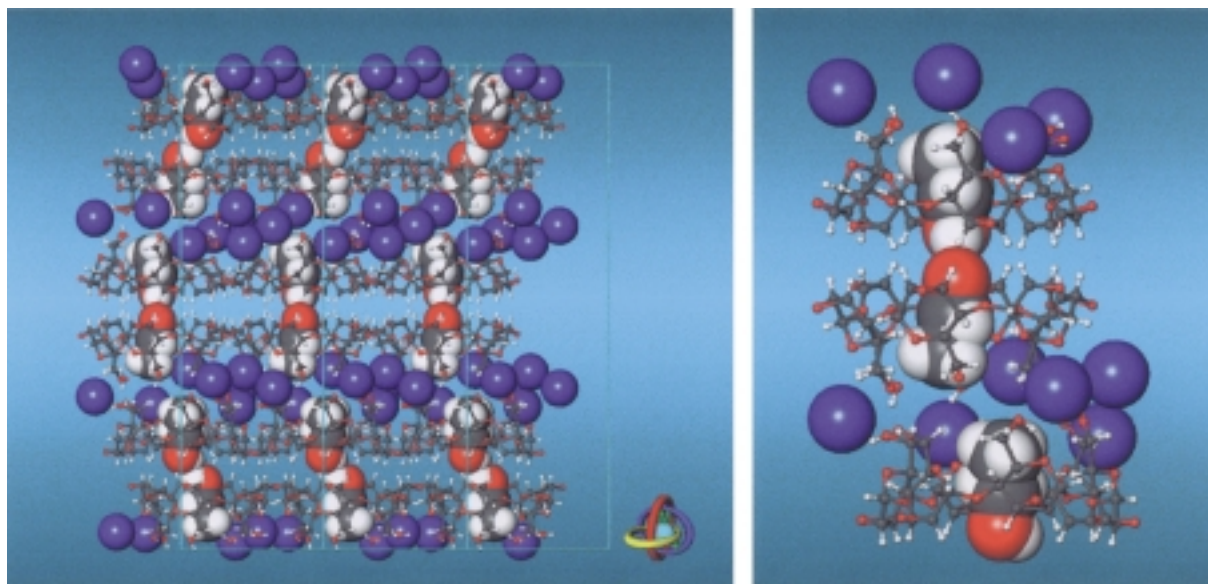


Figure 3. Assembly of the 2,3-anhydro- α -cyclomannin (**4**)–ethanol·3.5H₂O complex in the crystal lattice: layers of head-to-head attached dimers of the macrocycle, held together by hydrogen bonding between the hydroxyl groups of two cavity-entrapped ethanol molecules, are separated by a layer of water molecules (blue spheres), which engage in hydrogen bonding with the primary 6-CH₂OH groups at the narrow rim of the macrocycle.

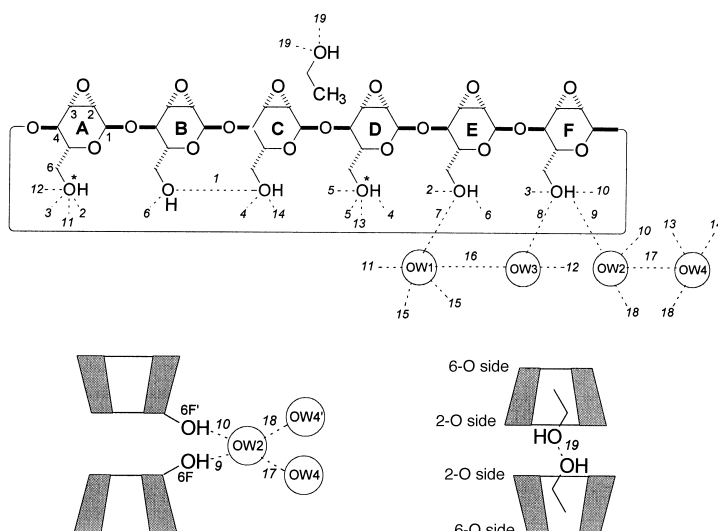


Figure 4. Scheme of intra- and intermolecular hydrogen bonds (top) in the solid-state structure of the 2,3-anhydro- α -cyclomannin–ethanol complex (**4**·EtOH). The individual 2,3-anhydro-mannose residues are labeled A–F and the disordered groups O(6A) and O(6D) are marked with “*”; of the four water positions OW1–OW4 the molecule OW2 is located on a symmetry element. The numbers in italics correspond to the indices given in Table 2; “open-ended” lines indicate H-bonds formed between symmetry related positions: The ethanol guest forms a single hydrogen bond to its symmetry image. The bottom schemes visualize the H-bonding pattern between O(6F) of two stacked cyclomannins and the intercalated OW2 and OW4 molecules, as well as the hydrogen bond formed between two ethanol guest molecules.

plausibility considerations already indicate, that a “replacement” of the hydrophilic secondary hydroxyl face of α -cyclodextrin^[2, 16] by a torus carrying epoxide rings should lead to a distinct decrease in hydrophilicity, inasmuch as the oxirane hydrogens H-2 and H-3 are placed at the rim’s upper side. Hence, the hydrophobic nature of the cavity of **4** is expected to extend sizably towards the oxirane ring-bearing

aperture, which in turn should lead to an increase in its capacity—as compared with α -CD—for inclusion complexation.

As lucidly borne out by the molecular lipophilicity pattern (MLP) of **4**, generated with the MOLCAD program^[14] and visualized by projection onto the contact surface of Figure 2 in color-coded form^[15] (cf. Figure 5), the macrocycle even has a lipophilicity distribution inverse to that of α -CD: The most hydrophobic (yellow) are located at the wider, oxirane ring-carrying torus, obviously due to the 2-H and 3-H ring protons of the sugar units forming its rim, and inside the cavity, whereas the hydrophilic (blue) domains are centered on the opposite side around the 6-hydroxyl groups.

Surprising, at first sight, is the fact, that the hydrophilic and hydrophobic surface regions at the guest–host interface are non-complementary: The hydrophilic region of the included ethanol (i.e., its hydroxyl end) is located at the hydrophobic oxirane ring-carrying opening of the macrocycle, whereas the hydrophilic regions of the host surround the guest’s ethyl group. This impression, however, only holds for the “isolated” monomeric macrocycle with its guest. Inspection of the de facto head-to-head dimer realized in the crystal lattice, reveals a higher order of complementarity between hydrophilic and hydrophobic surface regions (Figure 6): not a guest–host and guest–guest correspondence—an assembly obviously augmented by a distinct OH...O hydrogen bond between two entrapped ethanol molecules. This unique arrangement entails the outside of the dimeric complex to be largely hydrophilic, hence capable of being embedded, as horizontal stacks, into layers of water (Figure 3).

Nevertheless, the question remains why the ethanol guest in this supramolecular assembly does not place itself in the cavity in an inverse way, that it faces the hydrophilic torus rim with its hydroxyl group as this would have the advantage of allowing hydrogen bonding to one of the 6-CH₂OH groups or

Table 2. Hydrogen-bond patterns in the solid-state structure of the 2,3-anhydro- α -cyclomannin–ethanol complex (**4**·EtOH), listed for distances $d(\text{H}\cdots\text{O}) < 2.5 \text{ \AA}$ and/or $d(\text{O}\cdots\text{O}) < 3.5 \text{ \AA}$ only; the water molecules are labeled OW1–OW4, the mannose labeling A–F and the indices given in the first column correspond to Figure 4.

No. (cf. Figure 4)	Hydrogen bond	$d(\text{H}\cdots\text{O})$ [\AA] ^[a]	$d(\text{O}\cdots\text{O})$ [\AA]	$\varphi(\text{OH}\cdots\text{O})$ [$^\circ$] ^[a]	Symmetry
intramolecular host–host hydrogen bonds:					
1	O(6B)⋯O(6C)	–	3.198	–	[b]
intermolecular host–host hydrogen bonds:					
2	O(6A1)⋯O(6E)	–	3.255	–	[c]
3	O(6A2)⋯O(6F)	–	2.838	–	[c]
4	O(6D1)H⋯O(6C)	1.845	2.586	149.5	[c]
5	O(6D2)⋯O(6D2)	–	2.662	–	[c]
6	O(6E)H⋯O(6B)	2.177	2.695	121.2	[c]
host–water hydrogen bonds:					
7	O(6E)⋯O(W1)	–	2.662	–	[b]
8	O(6F)⋯O(W3)	–	3.156	–	[b]
9	O(6F)H⋯O(W2)	2.145	2.871	147.4	[b]
10	O(6F)H⋯O(W2)	2.146	2.872	147.4	[c]
11	O(6A1)⋯O(W1)	–	2.917	–	[c]
12	O(6A2)⋯O(W1)	–	2.970	–	[c]
12	O(6A2)⋯O(W3)	–	2.894	–	[c]
13	O(6D1)⋯O(W4)	–	3.225	–	[d]
14	O(6C)⋯O(W4)	–	3.324	–	[e]
water–water hydrogen bonds:					
15	O(W1)⋯O(W1)	–	2.785	–	[f]
16	O(W1)⋯O(W3)	–	2.444	–	[b]
17	O(W2)⋯O(W4)	–	2.950	–	[b]
18	O(W2)⋯O(W4)	–	2.949	–	[c]
guest–guest hydrogen bonds:					
19	O(1)⋯O(1)	–	3.025	–	[g]

[a] Hydrogen-bond H⋯O distances and O–H⋯O angles omitted if hydrogen atoms were not located explicitly, labels O(6A1), O(6A2), O(6D1), and O(6D2) indicate disordered positions. Symmetry operations: [b] x, y, z ; [c] $x, x - y, -z$; [d] $x + 1, y, z$; [e] $x + 1, x - y + 1, -z$; [f] $x, x - y - 1, -z$; [g] $-y, -x, -z + 1/3$.

Table 3. Selected intermolecular heavy atom distances in solid-state structure of the 2,3-anhydro- α -cyclomannin–ethanol complex (**4**·EtOH); labeling of the mannose units corresponds to Figure 4 and Table 2. For additional parameters on host–water distances see the list of hydrogen bonds given in Table 2.

Distances ^[a] ($d < 3.3 \text{ \AA}$)	d [\AA]	sym- metry	distances ^[a]	d [\AA]	sym- metry
host–host (layered):			host–guest:		
C(3D)⋯O(2A)	3.215	[d]	O(1)⋯O(1B)	4.188	[g]
C(4D)⋯O(2A)	3.270	[d]	O(1)⋯C(2C)	4.197	[g]
C(1C)⋯O(2A)	3.185	[d]	O(1)⋯C(3C)	3.979	[g]
O(2D)⋯C(3A)	3.173	[d]	O(1)⋯O(1)	4.68(15) ^[h]	[b]
O(2D)⋯C(4A)	3.236	[d]	O(1)⋯C(2)	5.54(20) ^[h]	[b]
O(2D)⋯C(1F)	3.234	[d]	O(1)⋯C(3)	5.40(15) ^[h]	[b]
C(3E)⋯O(2B)	3.152	[e]	C(1)⋯O(1)	4.39(40) ^[h]	[b]
C(4E)⋯O(2B)	3.201	[e]	C(1)⋯C(5)	4.46(39) ^[h]	[b]
O(2E)⋯C(3B)	3.156	[e]	C(2)⋯O(1)	4.57(16) ^[h]	[b]
O(2E)⋯C(4B)	3.175	[e]	C(2)⋯C(5)	4.19(27) ^[h]	[b]
host–host (stacked):			guest–guest:		
C(6E)⋯O(6A1)	3.204	[c]	O(1)⋯O(1)	3.025	[g]
O(6C)⋯C(6D1)	3.229	[c]	C(2)⋯C(2)	6.821	[c]
O(2F)⋯C(2F)	3.290	[f]			
O(2F)⋯O(2F)	3.297	[f]			

[a] Disordered positions are indicated by the labels O(6A1), O(6A2), O(6D1), and O(6D2). Symmetry operations: [b] x, y, z ; [c] $x, x - y, -z$; [d] $x + 1, y, z$; [e] $x, y - 1, z$; [f] $-y + 1, -x + 1, -z + 1/3$; [g] $-y, -x, -z + 1/3$; [h] Parameters averaged over all equivalent host–guest distances (e.g., distances EtOH⋯O1A–F) with root-mean-square deviations in parenthesis.

to a water molecule in the then adjoining water layer. On the other hand, though, this would conceivably create a “hydrophobic void” in the cavity as the ethyl portion of the guest is not long enough to fill it entirely. If this notion is correct,

higher alcohols are likely to form inclusion complexes with 2,3-anhydro- α -cyclomannin in which the orientation of the guests is inverse to that of ethanol.

Conclusion

The solid-state structure of the 2,3-anhydro- α -cyclomannin–ethanol–water inclusion complex detailed herein provides a unique example of crystal engineering,^[17] as three structurally divers components assemble—with an amazing level of precision^[18]—to a super-structure by mutual recognition of their steric, polar and non-polar features, the major directional force in its supramolecular construction undoubtedly being an optimal use of their hydrogen bonding capabilities.

Particularly intriguing is the finding that the 2,3-anhydro-cyclomannin host—lacking secondary hydroxyl groups at the wider torus, with which cyclodextrins form dimers via an intense hydrogen-bonding network—nevertheless finds a means to associate to dimers, that is via OH⋯OH hydrogen bonding between the ethanol guests, which is only possible though, when they are incorporated into the host in a “mismatch” of hydrophobic and hydrophilic surface regions at the guest–host interface. Thus, it is conceivable, that higher alcohols or phenols are being incorporated into the cavity of **4** in an inverse orientation with a more optimal complementarity of non-covalent guest–host interaction. As the 1-propanol inclusion complex of **4** has been obtained crystalline, the factors underlying the interplay of steric, polar, and non-

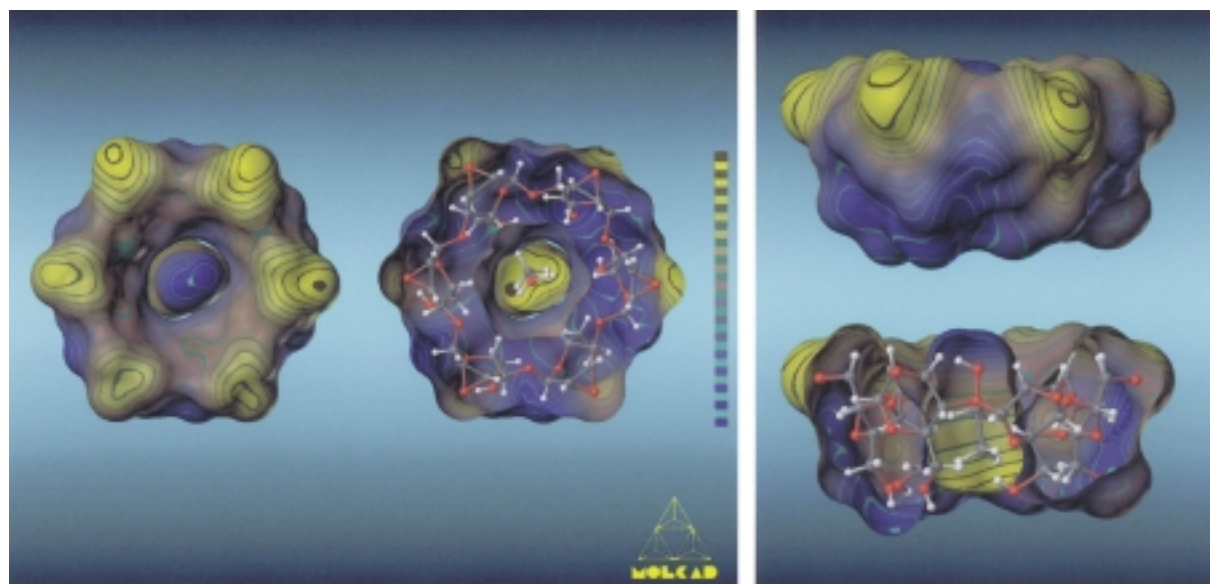


Figure 5. Molecular lipophilicity patterns (MLPs) of the 2,3-anhydro- α -cyclomannin ethanol complex (**4**·EtOH): The relative hydrophobicity of guest and host were mapped in color-coded form onto their individual contact (i.e., solvent-accessible) surfaces, with the colors ranging from dark-blue (most hydrophilic areas) to yellow–brown (hydrophobic domains). Application and scaling of the MLPs was done for guest and host separately followed by reassembly of the complex. Left: View onto the wider opening of the macrocycle carrying the six oxirane rings, displaying the hydrophobic (yellow) side. The front-opened version (center) with ball-and-stick model insert exposes the distinctly hydrophilic (blue) rear side bearing the 6-CH₂OH groups. Right: The side view representations clearly illustrate the apparent non-complementarity of hydrophobic and hydrophilic regions of guest–ethanol and host, the hydrophilic ethanol-OH group being located at the lipophilic side of the cavity.

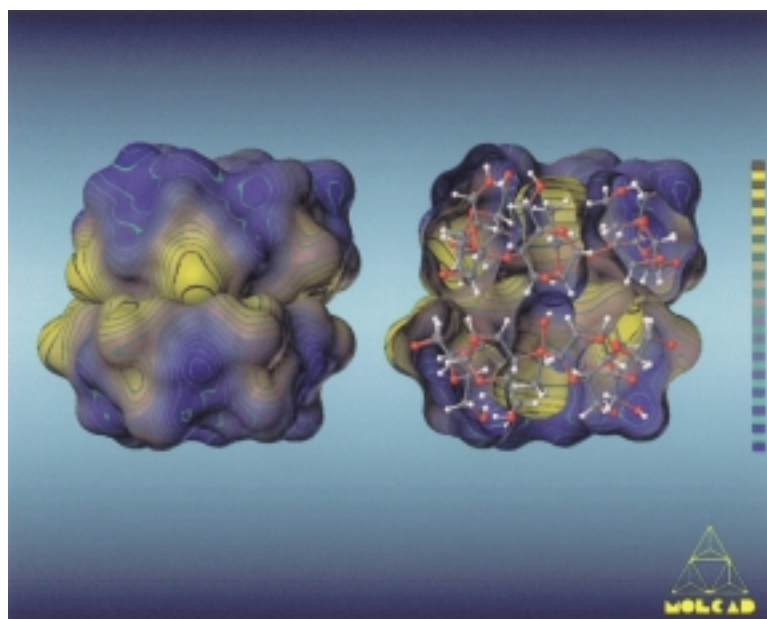


Figure 6. Molecular lipophilicity patterns (MLPs) of one dimeric unit of the 2,3-anhydro- α -cyclomannin–ethanol complex (**4**·EtOH) as excised from the crystal lattice. Although a “mismatched” host–guest arrangement in terms of relative hydrophobicity is observed for the monomer (cf. Figure 5), the “matching” interactions become obvious in the “head-to-head” dimer: the cohesion of two macrocycles via their hydrophobic domains at the wider, oxirane-ring carrying torus is augmented by the distinct OH...O hydrogen bond between the oxygens of the entrapped ethanol molecules, facing each other via their hydrophilic surface areas. This reciprocal complementarity of hydrophobic (host–host) and hydrophilic (guest–guest) surface regions entails the outside of the dimeric assembly to be largely hydrophilic; in the crystal lattice it packs into horizontal layers that are separated by water (cf. Figure 3).

covalent interactions between its structurally as diverse components as **4**, a suitable guest, and notably, water are being probed further.

Experimental Section

General: All reactions were monitored by thin-layer chromatography on aluminum plates coated with silica gel 60 F₂₅₄. Melting points are uncorrected. ¹H- and ¹³C-NMR spectra were determined on a Varian Unity plus 500 spectrometer. FAB-MS were recorded on a JEOL JMS-DX 303 instrument.

Per-6-*O*-*tert*-butyldimethylsilyl-2,3-anhydro- α -cyclomannin [cyclohexakis-6-*O*-*t*-butyldimethylsilyl-(1 → 4)-2,3-anhydro- α -D-mannopyranosyl] (3): Per-6-*O*-(*t*-butyldimethylsilyl)- α -cyclodextrin (**2**, 1.0 g, 0.6 mmol),^[10] was added to a solution of NaH (0.40 g, 10.8 mmol) in anhydrous DMF (40 mL) and the mixture was kept under N₂ at 60 °C for 2 h. After cooling, benzenesulfonyl chloride (568 μ L, 4.32 mmol) in anhydrous DMF (10 mL) was injected followed by stirring at room temperature for 30 min. Filtration and flash chromatography on a silica gel column (4 × 15 cm) with benzene/EtOAc 4:1 (250 mL) afforded **3** (600 mg, 64%); m.p.: 203 °C (decomp.); [α]_D²⁰ = +70.1 (*c* = 0.36 in THF). ¹H NMR (500 MHz, CDCl₃, relevant data): δ = 3.11 (d, 1H, 2-H), 3.32 (d, 1H, 3-H), 3.56 (d, 1H, 5-H), 3.64, 3.93 (2d, 1H), 6-H₂), 4.24 (d, 1H, 4-H), 5.16 (s, 1H, 1-H), $J_{1,2} = J_{3,4} = 0$, $J_{2,3} = 3.7$, $J_{4,5} = 11.5$ Hz; ¹³C NMR (125 MHz, CDCl₃): δ = −5.17, −4.96 (*Me*₂Si), 18.31 (*t*BuCSi), 25.91 (*t*BuMe₃), 49.15 (C-2), 53.30 (C-3), 62.17 (C-6), 68.43 (C-4), 69.74 (C-5), 96.69 (C-1); MS [*M*]⁺ not detectable; C₇₂H₁₃₂O₂₄Si₆ (1550.2): C 55.78, H 8.58; found: C 55.55, H 8.68.

Per-2,3-anhydro- α -cyclomannin–ethanol inclusion complex [cyclohexakis-(1 → 4)-2,3-anhydro- α -D-mannopyranosyl–ethanol] (4·EtOH): A 1M solution of Bu₄NF in THF (4.6 mL) was added to a solution of silyl epoxide **3** (1.0 g, 0.65 mmol) in anhydrous THF (90 mL) under N₂, and the mixture was stirred at 40 °C for 4 h. Concentration in vacuo gave a syrupy residue, which was dissolved in commercially available 95 % EtOH (10 mL).

Standing overnight in a refrigerator resulted in a precipitate which was collected and dried in vacuo over P_2O_5 at ambient temperature for 24 h: **4**·EtOH (511 mg, 84%); m.p.: 267 °C (partial melting with browning, followed by gradual decomp.); $[\alpha]_D^{25} = +87$ ($c = 0.3$ in DMSO). 1H NMR (500 MHz, $[D_5]$ pyridine): $\delta = 3.47$ (d, 1H, 2-H), 3.73 (d, 1H, 3-H), 4.18, 4.43 (2m, 1H, 6-H₂), 4.34 (m, 1H, 5-H), 4.40 (d, 1H, 4-H), 5.63 (s, 1H, H-1), $J_{1,2} = J_{3,4} = 0$, $J_{2,3} = 3.5$, $J_{4,5} = 9.0$ Hz, assignments were substantiated by 1H – 1H and 1H – ^{13}C 2D NMR; ^{13}C NMR (125 MHz, $[D_5]$ pyridine): $\delta = 49.61$ (C-2), 54.03 (C-3), 62.81 (C-6), 70.10 (C-4), 71.27 (C-5), 96.37 (C-1); FAB-MS: m/z : 865 $[M]^+$; $C_{36}H_{48}O_{24} \cdot C_2H_5OH \cdot 2H_2O$ (944.8): C 48.30, H 6.18; found: C 48.14, H 6.11.

Crystals suitable for X-ray analysis were grown by suspending **4**·EtOH (10 mg) in 95% ethanol (5 mL), followed by brief warming to 65 °C, filtration through a membrane filter, and standing of the filtrate at room temperature for about a week. Of the crystals obtained (3 mg) a colorless prism with dimensions of $0.75 \times 0.4 \times 0.4$ mm was suited for X-ray exposure, its composition being $C_{36}H_{48}O_{24} \cdot C_2H_5OH \cdot 3.5H_2O$ ($M_r = 973.89$). It had space group $P3_12$, trigonal, with $a = b = 14.076(6)$, $c = 41.610(10)$ Å; $V = 7139.8(46)$ Å³, $Z = 6$, $\rho = 1.349$ g cm⁻³, $\mu(MoK\alpha) = 0.110$ mm⁻¹, $T = 293(2)$ K. A total of 8154 reflections were collected on a Enraf–Nonius CAD-4 diffractometer with graphite-monochromated $MoK\alpha$ ($\lambda = 0.71093$ Å) radiation, of which 5104 were independent ($R_{int} = 0.1537$). The structure was solved by direct methods (SHELXS-86^[20]) and successive Fourier difference synthesis. Refinement (on F^2) was performed by full-matrix least squares method with SHELXL-93^[20] $R(F) = 0.1069$ for 4036 reflections with $I \geq 2\sigma I$, $\omega R(F^2) = 0.2890$ for all 5104 reflections with $\omega = 1/(\sigma^2(F_o^2) + (0.0205P)^2 + 3.4693P)$; where $P = (F_o^2 + 2F_c^2)/3$. The 6-CH₂OH groups of two 2,3-anhydro-mannoside units diametrically across the macroring are disordered over two positions with occupancies of 50%, respectively (torsion angles $\omega(O5-C5-C6-O6) \approx +70^\circ$ and -60°). All non-hydrogen atoms except the disordered carbon atoms were refined anisotropically; hydrogen atoms on the 2,3-anhydro- α -cyclomannin were considered in calculated positions with the $1.2 \times U_{eq}$ value of the corresponding bound atom. The hydroxyl proton of the ethanol was subsequently positioned geometrically.

Crystallographic data (excluding structure factors) for the **4**·EtOH have been deposited with the Cambridge Crystallographic Data Centre as supplementary publication no. CCDC-143714. Copies of the data can be obtained free of charge on application to CCDC, 12 Union Road, Cambridge CB21EZ, UK (fax: (+44)1223-336-033; e-mail: deposit@ccdc.cam.ac.uk).

Computational details: Calculation of the molecular contact surfaces and the respective hydrophobicity potential profiles (MLP's) was performed using the MOLCAD molecular modeling program.^[14, 15] Scaling of the MLP profiles was performed in relative terms (most hydrophilic to most hydrophobic surface regions); no absolute values are displayed. Molecular Graphics were generated using MolArch⁺.^[21]

Acknowledgement

Financial support was provided by the Fonds der Chemischen Industrie. In addition, we thank Mrs. Sabine Foro for collecting the X-ray crystallographic data, Prof. Dr. J. Brickmann, Institut für Physikalische Chemie of this University, for access to the MOLCAD software package, and to the Japan Maize Products Co. Ltd. for providing α -cyclodextrin.

- [1] For reviews, see: a) F. W. Lichtenthaler, S. Immel, *J. Inclusion Phenom. Mol. Recognit. Chem.* **1996**, *5*, 3–16; b) G. Gattuso, S. A. Nepogodiev, J. F. Stoddart, *Chem. Rev.* **1998**, *98*, 1930–1958.
- [2] F. W. Lichtenthaler, S. Immel, *Tetrahedron: Asymmetry* **1994**, *5*, 2045–2060.
- [3] a) A. W. Coleman, P. Zhang, C. C. Ling, J. Mahuteau, H. Parrot-Lopez, M. Miocque, *Supramol. Chem.* **1992**, *1*, 11–14; b) P. Zhang, A. W. Coleman, *Supramol. Chem.* **1993**, *2*, 255–263.
- [4] Y. Nogami, K. Nasu, T. Koga, K. Ohta, K. Fujita, S. Immel, H. J. Lindner, G. E. Schmitt, F. W. Lichtenthaler, *Angew. Chem.* **1997**, *109*, 1987–1991; *Angew. Chem. Int. Ed. Engl.* **1997**, *36*, 1899–1902.
- [5] Nomenclature: a) According to a recent proposal for a simplified designation of non-glucose cyclooligosaccharides^[2, 5b] which has been authoritatively endorsed,^[5c] the mannose analogue of α -cyclodextrin is termed α -cyclomannin; as **4** is the 2,3-anhydro derivative thereof, we prefer, for practical reasons, the term 2,3-anhydro- α -cyclomannin^[4] rather than cyclo- α -1,4-hexamanno-2,3-epoxide, also used previously.^[5] The systematic name required by recent IUPAC recommendations (*Carbohydr. Res.* **1997**, *297*, 79, Rule 2-Carb-374.2) turns out to be *cyclohexakis-(1 → 4)-2,3-anhydro- α -D-mannopyranosyl*, which is not only less handy, but inconsistent, since **4** is not a series of “glycosyls”, but a glycoside, a hexasaccharide, in fact. To comply with the rules, the experimental section features both versions; b) S. Immel, J. Brickmann, F. W. Lichtenthaler, *Liebigs Ann. Chem.* **1995**, 929–942; c) J. Szejtli, in *Comprehensive Supramolecular Chemistry, Vol. 3 (Cyclodextrins)* (Eds.: J. Szejtli, T. Osa), Pergamon, Oxford, UK, **1996**, p. 7; J. Szejtli, *Chem. Rev.* **1998**, *98*, 1743–1754.
- [6] a) P. R. Ashton, C. L. Brown, S. Menzer, S. A. Nepogodiev, J. F. Stoddart, D. J. Williams, *Chem. Eur. J.* **1996**, *2*, 580–591; b) P. R. Ashton, S. J. Cantrill, G. Gattuso, S. Menzer, S. A. Nepogodiev, A. N. Shipway, J. F. Stoddart, D. J. Williams, *Chem. Eur. J.* **1997**, *3*, 1299–1314.
- [7] a) α -Cycloaltrin: [4]; b) α -Cycloaltrin: K. Fujita, H. Shimada, K. Ohta, Y. Nogami, K. Nasu, *Angew. Chem.* **1995**, *107*, 1783–1784; *Angew. Chem. Int. Ed. Engl.* **1995**, *34*, 1621–1622; c) α -Cycloaltrin: Y. Nogami, K. Fujita, K. Ohta, K. Nasu, H. Shimada, C. Shinohara, T. Koga, *J. Inclusion Phenom. Mol. Recognit. Chem.* **1996**, *25*, 53–56.
- [8] S. Immel, K. Fujita, F. W. Lichtenthaler, *Chem. Eur. J.* **1999**, *5*, 3185–3192.
- [9] It has been stated,^[3a] albeit without any preparative or spectroscopic proof, that 2,3-anhydro- α -cyclomannin gives 1:1 complexes with anethole, vanillin, and *N*-acetylphenylalanine.
- [10] K. Takeo, K. Uemura, H. Mitoh, *J. Carbohydr. Chem.* **1988**, *7*, 293–308.
- [11] The tilt angle $\tau^{[1b, 4]}$ is defined as the angle between the least-squares best-fit mean-plane of the macrocycle (all O-1 atoms) and each pyranose ring (atoms C-1 through C-5 and O-5).
- [12] a) D. A. Cremer, J. A. Pople, *J. Am. Chem. Soc.* **1975**, *97*, 1354–1358; b) G. A. Jeffrey, R. Taylor, *Carbohydr. Res.* **1980**, *81*, 182–183.
- [13] X. Wu, F. Kong, D. Lu, G. Li, *Carbohydr. Res.* **1992**, *235*, 163–178.
- [14] a) J. Brickmann, *MOLCAD—MOlecular Computer Aided Design*, Technical University of Darmstadt, **1996**; J. Brickmann, *J. Chim. Phys.* **1992**, *89*, 1709–1721. The major part of the MOLCAD program is included in the SYBYL package of TRIPOS Associates, St. Louis, USA; b) J. Brickmann, T. Goetze, W. Heiden, G. Moeckel, S. Reiling, H. Vollhardt, C.-D. Zachmann, *Interactive Visualization of Molecular Scenarios with the MOLCAD/SYBYL Package*, in *Data Visualization in Molecular Science: Tools for Insight and Innovation* (Ed.: J. E. Bowie), Addison-Wesley Publ., Reading, Mass., USA, **1995**, pp. 83–97; c) M. Teschner, C. Henn, H. Vollhardt, S. Reiling, J. Brickmann, *J. Mol. Graphics* **1994**, *12*, 98–105.
- [15] a) W. Heiden, G. Moeckel, J. Brickmann, *J. Comput. Aided Mol. Des.* **1993**, *7*, 503–514; b) S. Reiling, M. Schlenkrich, J. Brickmann, *J. Comput. Chem.* **1996**, *17*, 450–468.
- [16] S. Immel, F. W. Lichtenthaler, *Liebigs Ann.* **1996**, 27–36.
- [17] G. R. Desiraju, *Angew. Chem.* **1995**, *107*, 2541–2558; *Angew. Chem. Int. Ed. Engl.* **1995**, *34*, 2311–2327.
- [18] Diction borrowed from S. Dunitz, *Pure Appl. Chem.* **1991**, *63*, 177.
- [19] The 2,3-anhydro- α -cyclomannin of m.p.: 166 °C—defacto a misprint; correct value 266 °C—and $[\alpha]_D^{25} = +83.6$ ($c = 0.34$ in DMSO) mentioned in [4] was precipitated from methanol, and, thus, conceivably was the methanol inclusion complex of **4**. The same is likely to apply to the “cyclo- α -1,4-hexamanno-2,3-epoxide” (\equiv **4**) of m.p.: 268–269.5 °C and $[\alpha]_D^{25} = +128$ ($c = 1.0$ in DMF), prepared by exposure of per-2-O-tosyl- α -CD to $K_2CO_3/MeOH$ (6 h, 60 °C) and recrystallization of the product from water and then from methanol,^[5b] despite of the fact that its microanalytical data were interpreted as to contain neither solvent.
- [20] G. M. Sheldrick, *SHELXS-86 and SHELXL-93—Programs for Crystal Structure Solution and Refinement*, University of Göttingen, **1986** and **1993**.
- [21] S. Immel, *MolArch⁺—MOlecular ARCHitecture Modeling Program*, Technical University of Darmstadt, **1997**.

Received: August 18, 1999

Revised version: November 29, 1999 [F1986]